Optimized Pulse Pattern with Half-wave Symmetry for 5-Level Converter

Jonas Weires, Pedro Leal dos Santos, Steven Liu
Department of Electrical and Computer Engineering - LRS
TU Kaiserslautern
Gottlieb-Daimler-Straße 47
67663 Kaiserslautern, Germany
Email: sliu@eit.uni-kl.de

Keywords

≪Efficiency≫, ≪Harmonics≫ ,≪Optimization algorithm≫,≪Pulse Width Modulation (PWM)≫, ≪Grid-connected converter≫, ≪Multi-level converters≫

Abstract

In this paper, an Optimized Pulse Pattern is developed for a generic 5-Level Voltage Source Converter. The optimization process minimizes the current total harmonic distortion, while switching at the fundamental frequency. By relaxing the constraints to a half-period symmetry, a superior performance is obtained in comparison with existing solutions.

Introduction

Multilevel converters have become the enabling power conversion technology for enabling medium and high voltage in high power applications for the actual power grid and large motor drives. As a major research topic, several modulation techniques have been proposed to achieve the required output alternating voltage [1][2]. **Pulse Width Modulation (PWM)**-based techniques are preferred for multilevel converters with smaller number of voltages levels. At the expense of higher switching losses, low harmonic distortion is obtained. In opposite, other modulation techniques, as the **Nearest Level Control (NLC)**, switching at the fundamental frequency, fail to cope with required output voltage quality in most applications. In some applications, an additional Active Power Filter is required to mitigate harmonic content to ensure compliance with grid codes [3].

To counteract the problem of increasing harmonic distortion at low switching frequencies for converters with a low number of possible voltage levels the **Selective Harmonic Elimination (SHE)** has been developed. This technique focus on the elimination of a specific limited number of lower-order harmonics. Several formulations and algorithms have been developed in the last decades [4]. **Optimized Pulse Pattern (OPP)** is an alternative technique, eliminating not only specific harmonics, but minimizing the overall harmonic distortion [5]. OPP is based on an offline-calculation of the switching pattern with the help of optimization algorithms. Through this optimization process, the total harmonic distortion of the output current at low switching frequencies, down to the fundamental component, is greatly reduced. Consequently, both switching and conduction losses, due to lower harmonic distortion, are decreased and the overall system efficiency is increased. In high power applications even small improvements in transmission efficiency offer enormous potential for energy- and cost-savings.

The most common approach, i.e. **quarter-wave symmetry (QWS)**, imposes a strong symmetry constrain for every quarter of one period on the generated pattern. This restricts the range of solution and therefore the degree of freedom of the optimization. Investigations with reduced symmetry requirements have been done for **3-Level (3L)** patterns, in particular [6], while a derivation and an analysis for **5-Level (5L)** patterns with reduced symmetry have not been carried out yet. Whereby it already shows, that for

3L patterns, a reduction of the symmetry constrain leads to a significant improved harmonic distortion within certain modulation ranges [7]. In this paper the **half-wave symmetry (HWS)** is considered. The following work transfers the HWS concept to 5L patterns and a comparison with QWS 5L is provided. Furthermore an interesting variant of the HWS is derived which offers the performance of the QWS, but does not have any discontinuities within the switching angles and is thus ideally suited for integration into a linear controller concept.

Problem Formulation

An ideal multilevel three-phase converter is connected to a symmetrical three-phase grid, represented as in Fig.1. The grid is considered to be an ideal and symmetrical alternating voltage source of amplitude $\hat{U}_g$ and fixed angular frequency ω_1. Both filter and grid inductance with corresponding resistances are represented by L_{ac} and R_{ac}. For synchronous machines a further generalized OPP approach can be found in [8].

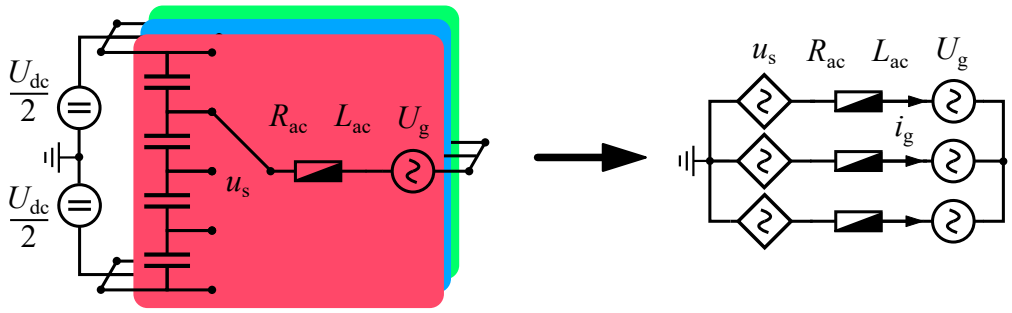

Fig. 1: Equivalent circuit of grid-connected converter

The optimization process intends to minimize the harmonic distortion of the output current i_g. The harmonic content of the output current is quantified by the **Total Demand Distortion (TDD)** and is used to derive the cost function:

$$I_{TDD} = \frac{1}{\sqrt{2} I_r} \cdot \sqrt{\sum_{h=2}^{h_{limit}} (\hat{i}_{g_h})^2} \tag{1}$$

Here I_r denotes the rated current of the converter (RMS) and h the harmonic order. The amplitudes of the current harmonic $\hat{i}_{g_h}$ can be expressed using the according output voltage harmonic amplitudes $\hat{u}_{s_h}$ of the converter:

$$\hat{i}_h = \frac{\hat{u}_{s_h}}{|Z_{ac_h}|} = \frac{\hat{u}_{s_h}}{\sqrt{{R_{ac}}^2 + (h\omega_1 L_{ac})^2}} \tag{2}$$

Neglecting the resistance ($R_{ac} \ll h\omega_1 L_{ac}$ for $h \gg 1$) and expressing the voltage harmonic amplitudes by normalized voltage amplitudes with $\hat{u}_{s_h} = \frac{U_{DC}}{2} \cdot \underline{\hat{u}}_{s_h}$ the equation can be written as:

$$I_{TDD} = \underbrace{\frac{U_{DC}}{\sqrt{2} I_r 2\omega_1 L_{ac}}}_{:=C} \cdot \sqrt{\sum_{h=2}^{h_{limit}} \left(\frac{\underline{\hat{u}}_{s_h}}{h} \right)^2} \tag{3}$$

The previously defined factor C contains only constant terms and therefore only scales the function. Furthermore, the square root is a strictly monotonically increasing function. Taking this into account and decomposing the normalized output voltage pattern with fourier series the cost function J can be derived:

$$J = \sum_{h=2}^{h_{limit}} \left(\frac{a_h^2 + b_h^2}{h^2} \right) \tag{4}$$

This general cost function is valid for all waveforms and symmetry conditions. Based on the respective waveform the fourier coefficients a_h and b_h are determined analytically and inserted into the objective function.

5L HWS OPP

The common QWS approach imposes not only QWS but also implicates HWS to the possible voltage pattern. Abolishing the strong QWS-constrain increases the degree of freedom for the optimization process. Thereby the HWS considers a half-wave period instead of only a quarter-wave period for optimization:

$$u_s(\pi+\omega t) = -u_s(\omega t) \tag{5}$$

The switching frequency of the switching units f_{SM} can be calculated by the number of switching angles per period $d_{2\pi}$ and the grid frequency $f_1 = \frac{\omega_1}{2\pi}$:

$$f_{SM} = \frac{d_{2\pi}}{2\cdot(L-1)}\cdot f_1 \overset{5L}{=} \frac{d_{2\pi}}{8}\cdot f_1 \tag{6}$$

Following the symmetry reduction, the number of switching angles, that are available for optimization, are doubled for HWS in comparison to QWS:

$$d_{QWS} = \frac{d_{2\pi}}{4} \qquad d_{HWS} = \frac{d_{2\pi}}{2} \tag{7}$$

The comparison between 5L QWS and 5L HWS can be seen in Fig.2 for fundamental switching with eight switching angles per period $d_{2\pi} = 8$.

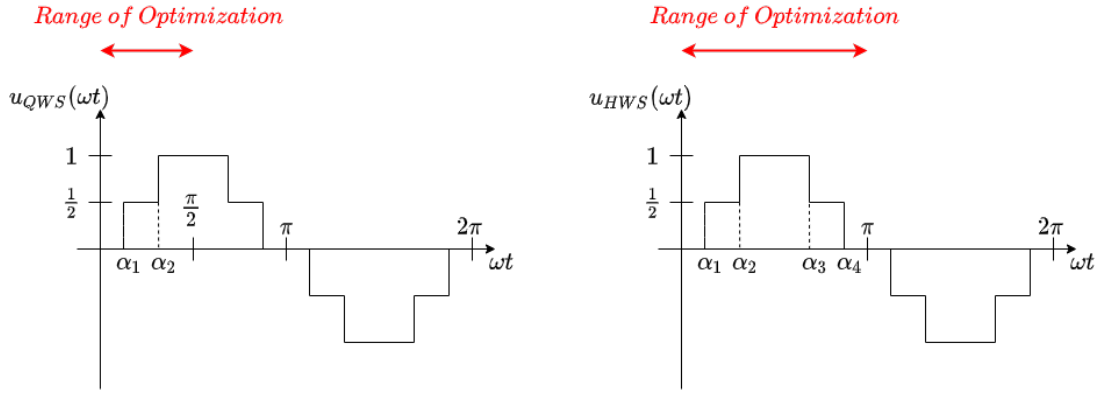

Fig. 2: Range of optimization QWS / HWS for fundamental switching $d_{2\pi} = 8$

Besides the number of switching transitions per period, the characteristic patterns are determined by the switching angles α_i with the corresponding switching transition Δu_{s_i} at the switching instance i. At each switching instance only one voltage step is allowed:

$$\Delta u_{s_i} \in \left\{-\frac{1}{2}, \frac{1}{2}\right\} \tag{8}$$

Regarding the normalized pattern the output voltage is then allowed to take the values:

$$u_{s_i} \in \left\{-1\,,\,-\frac{1}{2}\,,\,0\,,\,\frac{1}{2}\,,\,1\right\} \tag{9}$$

In addition to the general reduction of the symmetry, the requirements for the possible voltage values are also greatly relaxed. Where the traditional QWS approach only allows positive voltage values in the first half-wave, now arbitrary voltage values are allowed e.g. negative values in the first positive half-wave. Additional patterns accomplished by HWS are shown exemplary for fundamental switching in Fig.3.

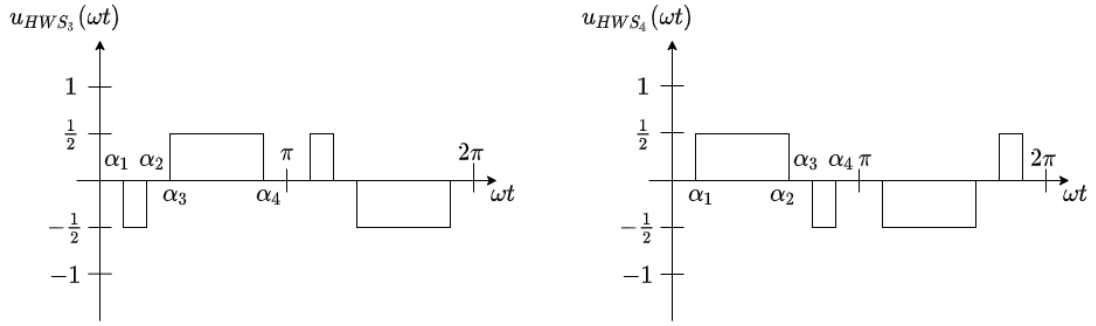

Fig. 3: Additional patterns 5L HWS $d_{2\pi} = 8$

To ensure that no further switching transitions at $\omega t = 0$ and $\omega t = \pi$ occur, the initial and end-value of the voltage pattern are restricted:

$$u_{s_0} = u_{s_{d_{HWS}}} = 0 \tag{10}$$

Due to the floating neutral point, common-mode voltages will not affect the current. Furthermore, as a result of the HWS, the amplitudes of even harmonics will be equal to zero. This leads to the final optimization problem, which considers two dimensions with switching angles $\boldsymbol{\alpha}$ and switching transition $\boldsymbol{\Delta u_s}$:

$$min\ J(\boldsymbol{\alpha}, \boldsymbol{\Delta u_s}) = \sum_{h=5,7,11,\ldots}^{h_{limit}} \left(\frac{a_h^2 + b_h^2}{h^2}\right) \tag{11}$$

$$subject\ to \quad a_1 = 0 \quad b_1 = m$$

$$0 \leq \alpha_1 \leq \alpha_2 \leq \ldots \leq \alpha_{d_{HWS}} \leq \pi$$

$$with \qquad \boldsymbol{\alpha} = [\alpha_1 \ldots \alpha_{d_{HWS}}]^T$$

$$\boldsymbol{\Delta u_s} = [\Delta u_{s_1} \ldots \Delta u_{s_{d_{HWS}}}]^T$$

The optimization problem is solved for fundamental switching i.e $d_{2\pi} = 8$ and the subsequent switching frequency with $d_{2\pi} = 12$. Assuming a grid frequency of $f_1 = 50Hz$ this leads to $f_{SM} = 50Hz$, $f_{SM} = 75Hz$

respectively. For low switching frequencies, and thus a low number of switching angles per period, it is suitable to reduce the two-dimensional optimization problem to a sum of one-dimensional optimization problems [9]. Therefor, all possible patterns are characterized by their combinations of transitions and determined in advance. Every combination of number of levels and number of switching angles per period leads to a characteristic set of possible patterns and the characterization has to be carried out again. In Table I an overview of the number of possible patterns for the considered combinations is provided.

Table I: Number of possible patterns

	3L QWS	5L QWS	5L HWS
$d_{2\pi} = 8$	1	2	4
$d_{2\pi} = 12$	1	2	14

Then for each pattern out of the set of possible patterns the global minimum of the non-linear non-convex optimization problem in the variable $\boldsymbol{\alpha}$ is found. In a final comparison the best solution among all patterns is selected and thus the optimal waveform with the corresponding switching angles for each modulation index m is determined. The optimization problem in the variable $\boldsymbol{\alpha}$ is solved numerically with the optimization tool fmincon of the Matlab software platform, which represents an implementation of **sequential quadratic programming (SQP)**. Due to the non-convex structure of the optimization problem locally converging methods like SQP are strongly dependent on the chosen initial value [8]. In order to be able to determine the global minimum, several calls of fmincon with different, randomly generated initial values are done. Finally the minima of all calls are compared and the best solution is selected. It should be noted here, that the minimum found is not necessarily a global minimum. However, if the number of calls is increased appropriately, the probability of finding the global minimum increases. In the optimization all harmonics up to the $100th$ order i.e. $n_{limit} = 100$ are considered. Furthermore, the modulation index m is represented with a resolution of $\Delta m = 0.01$ within the interval $m \in [0.01, 1.2]$. In Fig. 4 the concept of the complete algorithm is given and a comparison of the computation time for one iteration is provided. The computation time is normalized to the 3L QWS approach.

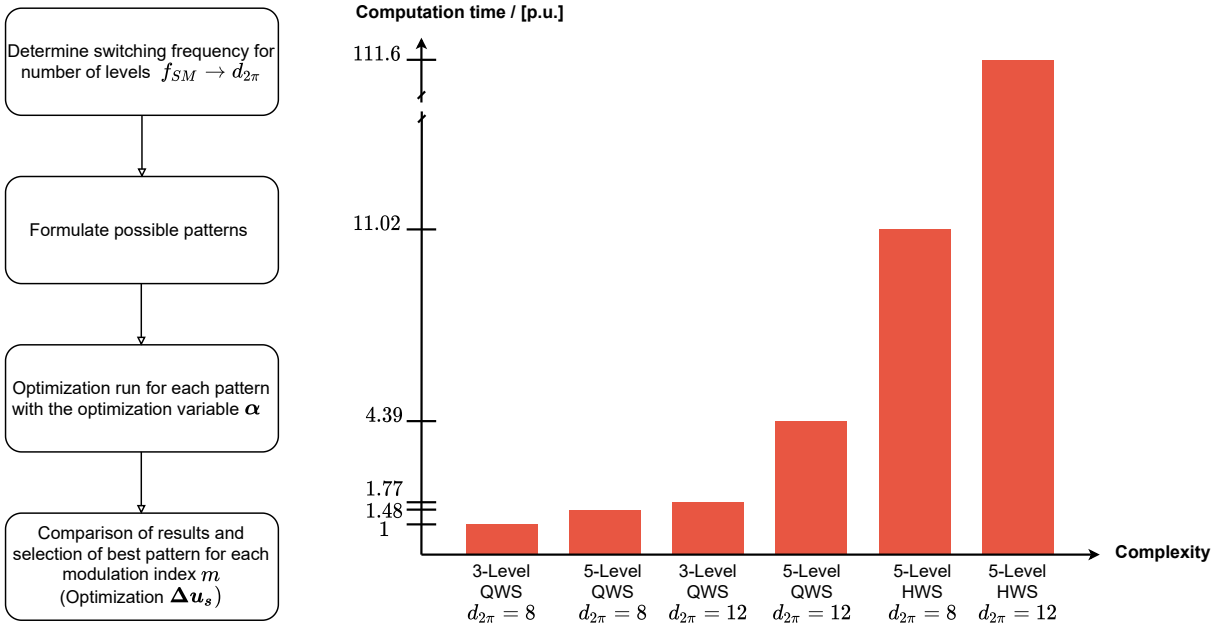

Fig. 4: Algorithm concept and computation time for one iteration

It can be seen that, with increasing degree of freedom, the complexity, and thus the calculation time, increases. Besides an increased calculation time per iteration, it becomes additionally more difficult to find the global minimum. Therefore the number of iterations, compared to 3L HWS [6], has to be increased

significantly to ensure that the global minimum is found. An Intel® Core™ i7-4790 Processor with 16GB RAM was used to run the algorithm. The 5L HWS with $d_{2\pi} = 12$ needed an overall computation time of 222 hours.

The harmonic distortion is directly calculated with the use of the fourier coefficients and displayed as **Total Harmonic Distortion (THD)**. In both cases the HWS provides improved harmonic distortion in numerous modulation ranges in direct comparison to the QWS. The results are shown in Fig.5. For $d_{2\pi} = 8$ the THD is reduced by up to 12.95% at $m = 0.38$. Furthermore, significant percentage improvements of the THD are obtained in ranges that are particularly relevant for grid-connected power converters. For example, the THD is reduced at the modulation-index of $m = 0.62$ with 10.77%. The reduction in harmonic distortion is particularly evident in the range $m \in [0.82, 0.9]$. Here the already very low THD values can be further reduced by up to 31.63% at $m = 0.87$.

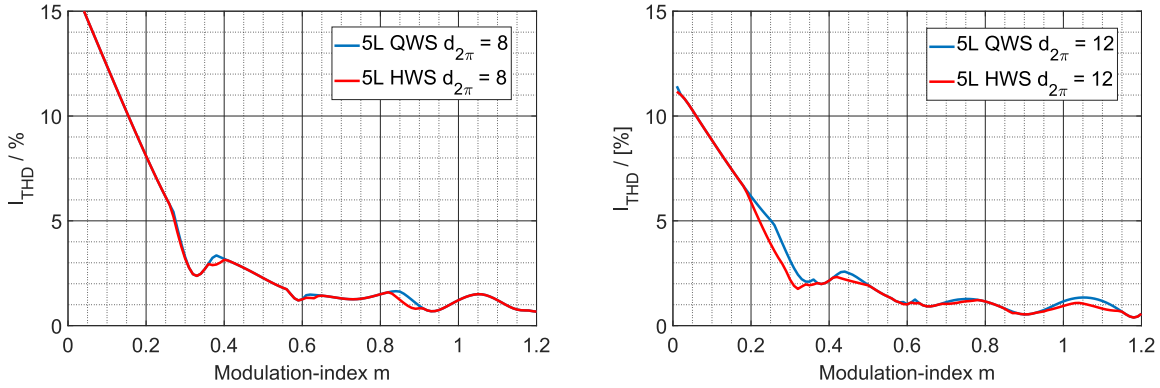

Fig. 5: Output current THD 5L QWS / 5L HWS

For $d_{2\pi} = 12$ it can be seen, that a reduction of the symmetry condition leads likewise to an improvement of the harmonic distortion over wide modulation ranges. Especially in the low modulation range there is a significant improvement by up to 25.68% at $m = 0.26$. Furthermore, within the range of $m \in [0.4, 0.5]$ there is a reduction of up to 14.39% at $m = 0.44$. At $m = 0.62$ an improvement of 14.92% is achieved. In the range of $m \in [0.68, 0.79]$ there is a reduction up to 12.11% at $m = 0.73$.

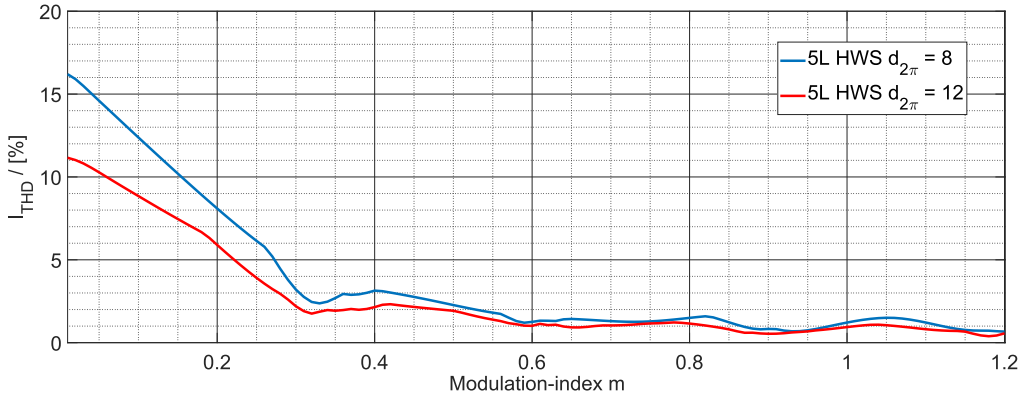

Fig. 6: Output current THD 5L HWS $d_{2\pi} = 8$ / 5L HWS $d_{2\pi} = 12$

In Fig. 6 the comparison for different number of switching angles per period for 5L HWS is given. It can be seen that an increased switching frequency leads to a reduced harmonic distortion. Overall, the 5L HWS leads to a significant reduction of harmonic distortion over numerous modulation ranges. Of particular importance is the lowest possible switching frequency of $f_{SM} = 50Hz$ with $d_{2\pi} = 8$. Here peak reductions of up to 31.63%, in particularly important operating ranges for power converters, can be achieved. As a result, the lowest possible switching frequency of $f_{SM} = 50Hz$ can be used without causing an excessive increase in THD. This leads to reduced switching losses and therefore improved

overall system efficiency. For simple verification, the designed 5L HWS was simulated in open-loop conditions against an inductive load. The results for two different operation points are shown in Fig. 7.

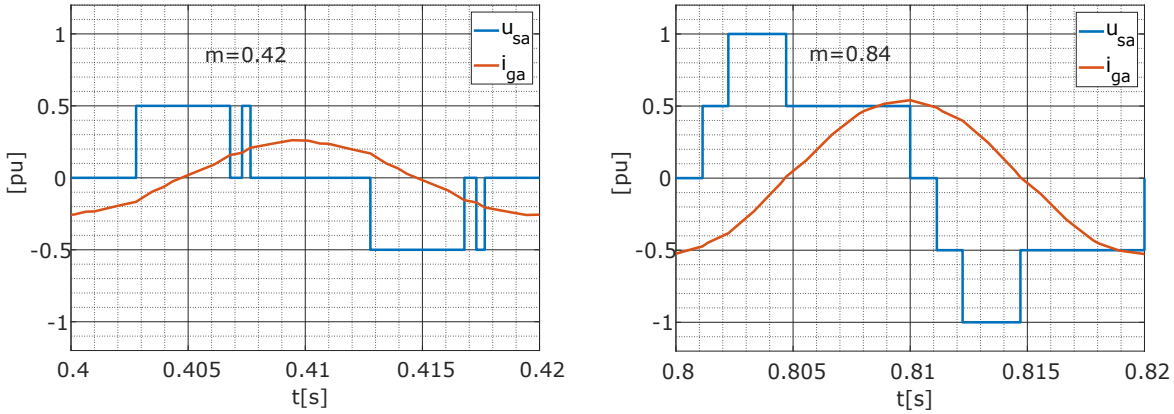

Fig. 7: Inverter voltage and output current 5L HWS $d_{2\pi} = 8$

5L HWS OPP with phase-shift

To further increase the degree of freedom and with it the solution range of the optimization the approach with allowed phase-shift is considered. It is basically based on the preceding approach. Hence, the computation regulation remains the same. The difference is given by adapted constraints. The fundamental component is now generally allowed to have a phase shift, i.e. both a_1 and b_1 can occur unequal zero. This leads to the constrain, that the amplitude of the fundamental component, resulting from the superposition of fundamental cosine and fundamental sine oscillation, must correspond to the modulation index:

$$\sqrt{a_1^2 + b_1^2} = m \tag{12}$$

The resulting phase-shift is determined after optimization and does not limit the optimization:

$$\tan(\phi_1) = \frac{a_1}{b_1} \tag{13}$$

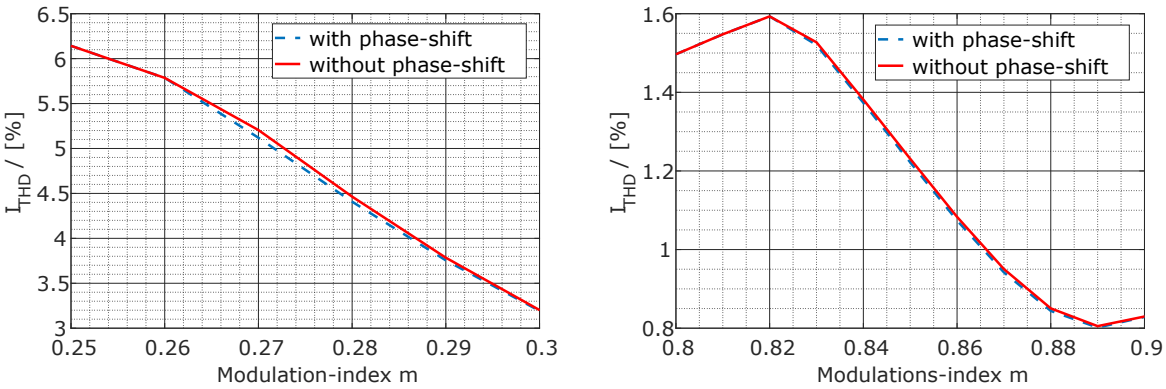

Fig. 8: Output current THD 5L HWS with / without phase-shift $d_{2\pi} = 8$

The optimization problem with allowed phase shift is now given by:

$$min\ J(\boldsymbol{\alpha}, \boldsymbol{\Delta u_s}) = \sum_{h=5,7,11,\ldots}^{h_{limit}} \left(\frac{a_h^2 + b_h^2}{h^2} \right) \tag{14}$$

$$subject\ to \quad \sqrt{a_1^2 + b_1^2} = m$$

$$0 \leq \alpha_1 \leq \alpha_2 \leq \ldots \leq \alpha_{d_{HWS}} \leq \pi$$

$$with \quad \boldsymbol{\alpha} = [\alpha_1 \ldots \alpha_{d_{HWS}}]^T$$

$$\boldsymbol{\Delta u_s} = [\Delta u_{s_1} \ldots \Delta u_{s_{d_{HWS}}}]^T$$

This optimization problem is now solved for the case $d_{2\pi} = 8$. The relevant patterns remain the same and only the constraint has to be adapted accordingly. The results and the comparison with the approach without phase-shift are shown in Fig.8 for the relevant modulation ranges. A closer look reveals a further improvement of the THD in the represented modulation ranges. However, the resulting phase shift has to be considered and increases the requirement for the superimposed control system and therefore overall system complexity.

5L HWS OPP with reduced Discontinuities

Based on the general HWS approach (11) an alternative method has been developed which addresses the OPP inherent problem of discontinuities within the switching angles. These discontinuities in the switching angles, when varying the modulation index, prevent the use of linear controllers due to stability issues [10] and are therefore ideally avoided in advance. For 5L HWS with $d_{2\pi} = 8$ exemplary discontinuities can be seen in the left side of Fig.9.

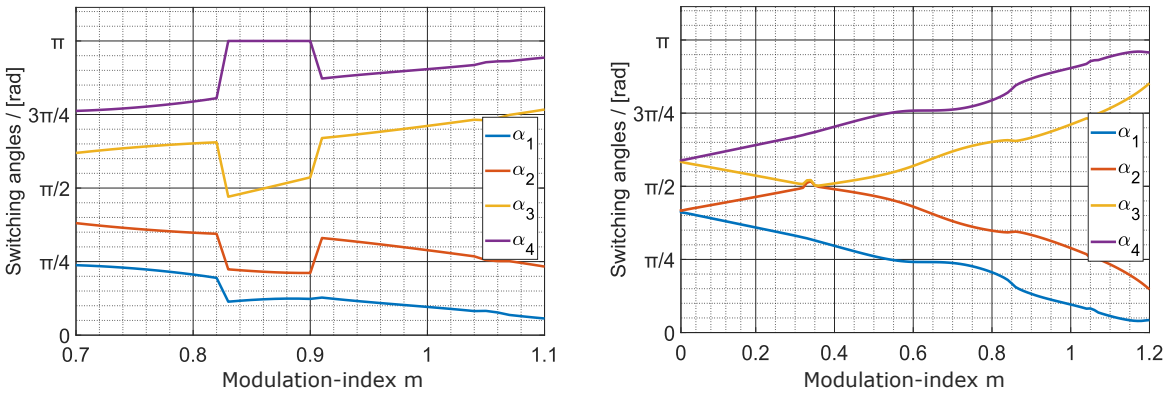

Fig. 9: 5L HWS with exemplary and reduced discontinuities $d_{2\pi} = 8$

Starting from the switching angles resulting for 5L HWS the ranges of discontinuities are regarded and specified. The possible range of values for each switching angle within the affected ranges are restricted, i.e. additional constrains are added to the optimization problem. These constrains have to be specified as minimal as possible to ensure the degree of freedom of the optimization remains as large as possible. For example for the discontinuity for α_4 in the range of $m \in [0.82, 0.91]$ the constrain is

given that $\alpha_4 < \pi$. Following this constrain, the solution of the optimization problem where α_4 forces a discontinuity can not be selected anymore, however a large searching area for a alternative solution is maintained. This process is carried out for every discontinuity of each switching angle. After the restriction process the optimization problem with additional constrains is solved and the switching angles are checked until the desired continuous course is achieved. This approach offers a greater flexibility compared to a directly in the solving algorithm implemented post-optimization loop as proposed in [11]. The course of the switching angles after the process can be seen in the right side of Fig.9. The method results in a continuous and smooth progression of the switching angles without any discontinuities.

The harmonic distortion in comparison to 5L QWS is shown in Fig.10. It can be seen that the harmonic distortion of the 5L HWS with reduced discontinuities corresponds over a wide working range to the harmonic distortion of the 5L QWS. Thus the increased degree of freedom from the HWS can be used to compensate for emerging constraints due to reduced discontinuities. Furthermore the smooth progression of the switching angles significantly reduces the increased harmonic distortion that occur in transient processes as a result of discontinuities. Accordingly, the requirements for the superimposed control system are decreased and the use of linear controllers is allowed.

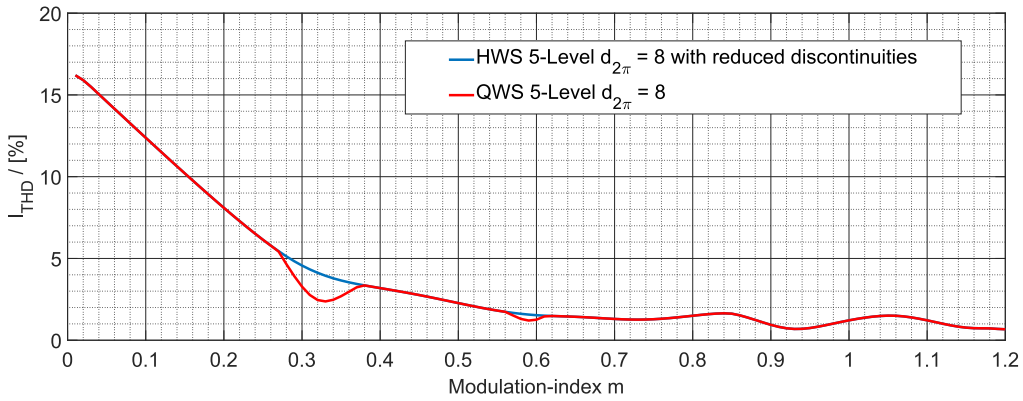

Fig. 10: Output current THD 5L QWS / 5L HWS with reduced discontinuities $d_{2\pi} = 8$

Conclusion

Reducing the symmetry constrain on the 5L OPP leads to significant improvements in harmonic distortion in several modulation ranges. Therefore 5L HWS OPP have superior performance compared to the common 5L QWS OPP. The increased degree of freedom can be used to avoid discontinuities under the expense of higher harmonic distortion. However, the harmonic distortion equals the performance of 5L QWS over a wide working range and therefore 5L HWS OPP can maintain the known harmonic distortion of 5L QWS with the advantage of smooth progression within the switching angles.

References

[1] A. A. Ferreira, C. C. Rodriguez and O. G. Bellmut: Modulation techniques applied to medium voltage modular multilevel converters for renewable energy integration: A review, Electric Power Systems Research, Volume 15, pp. 21-39, 2018

[2] P. dos Santos, M. Vazquez and S. Liu: Flexible and General Strategy of Space Vector Modulation for Multilevel Converters, PCIM Asia 2020 International Exhibition and Conference for Power Electronics, Intelligent Motion, Renewable Energy and Energy Management, pp. 1-7, 2020

[3] H. Wang and S. Liu: An optimal strategy with convex-concave constraints for power factor correction and harmonic compensation under different voltages, IEEE International Conference on Industrial Technology (ICIT), pp. 275-280, mar 2016

[4] M. S. A. Dahidah, G. Konstantinou and V. G. Agelidis: A Review of Multilevel Selective Harmonic Elimination PWM: Formulations, Solving Algorithms, Implementation and Applications, IEEE Transactions on Power Electronics, vol. 30, no. 8, pp. 4091-4106, aug 2015

[5] G. S.Buja and G. B. Indri: Optimal pulsewidth modulation for feeding AC motors, IEEE Transaction on Industrial Application, vol. IA-13, no. 1, pp. 38–44, jan 1977

[6] A. Birth, T. Geyer, H. du Toit Mouton, and M. Doring: Generalized three-level optimal pulse patterns with lower harmonic distortion, IEEE Transactions on Power Electronics, vol. 35, pp.5741 - 5752, jun 2020
[7] A. Birth, T. Geyer, and H. du Toit Mouton: Symmetry relaxation of three-level optimal pulse patterns for lower harmonic distortion, 2019 21st European Conference on Power Electronics and Applications (EPE 19 ECCE Europe), sep 2019
[8] N. Hartgenbusch, R. W. D. Doncker, and A. Thunen: Optimized pulse patterns for salient synchronous machines, 2020 23rd International Conference on Electrical Machines and Systems (ICEMS), nov 2020
[9] A. K. Rathore, J. Holtz, and T. Boller: Synchronous optimal pulsewidth modulation for low-switching-frequency control of medium-voltage multilevel inverters, IEEE Transactions on Industrial Electronics, vol. 57, pp. 2374 - 2381, jul 2010
[10] M. Vasiladiotis, A. Christe, and T. Geyer: Model predictive pulse pattern control for modular multilevel converters, IEEE Transactions on Industrial Electronics, vol. 66, pp. 2423 - 2431, mar 2019
[11] A. K. Rathore, J. Holtz, and T. Boller: Generalized optimal pulsewidth modulation of multilevel inverters for low-switching-frequency control of medium-voltage high-power industrial ac drives, IEEE Transaction on Industrial Electronics, vol. 60, no. 10, pp. 4215–4224, oct 2013